The New Madrid Seismic Zone: Not Dead Yet

Morgan T. Page* and Susan E. Hough

The extent to which ongoing seismicity in intraplate regions represents long-lived aftershock activity is unclear. We examined historical and instrumental seismicity in the New Madrid central U.S. region to determine whether present-day seismicity is composed predominantly of aftershocks of the 1811–1812 earthquake sequence. High aftershock productivity is required both to match the observation of multiple mainshocks and to explain the modern level of activity as aftershocks; synthetic sequences consistent with these observations substantially overpredict the number of events of magnitude ≥ 6 that were observed in the past 200 years. Our results imply that ongoing background seismicity in the New Madrid region is driven by ongoing strain accrual processes and that, despite low deformation rates, seismic activity in the zone is not decaying with time.

Seismic hazard is not isolated to tectonic plate boundaries, as evidenced by earthquakes that occur in stable continental regions. Intraplate earthquakes, which are related to the internal deformation of plates rather than motion at plate boundaries, can be large and damaging, as with the 2001 Bhuj earthquake (*1*). In this work, we study the 1811–1812 New Madrid sequence, which is of paramount importance for understanding intraplate seismogenesis and for probabilistic seismic hazard assessment in the central and eastern United States and other midcontinental regions. The sequence included four events that were widely felt throughout the central and eastern United States, conventionally regarded as three primary mainshocks and the large dawn aftershock following the first mainshock. Magnitude estimates for these events have varied widely, from a low of magnitude (M) ≈ 7 for the largest mainshocks (*2*) to values over 8 in magnitude (*3*).

Aftershocks of the 1811–1812 sequence have been considered in two ways. Several studies have used archival accounts of large aftershocks and/or tallies of felt earthquakes to estimate magnitudes for large aftershocks and consider the overall magnitude distribution of early aftershocks [e.g., (*4*, *5*)]. Two studies have considered the long-term rate of seismicity in the New Madrid Seismic Zone (NMSZ) and concluded that it is well characterized as a long-lived aftershock sequence (*6*, *7*). It is important to note, however, that these latter two studies do not show a fit, from 1811 to present, to traditional Omori decay (*8*, *9*). Such direct evidence has been observed for the classic long-lived aftershock sequence following the 1891 Nobi earthquake, for which an Omori decay can be seen for 100 years (*10*). In the New Madrid case, however, a direct fit is not possible given uncertainties in the early New Madrid catalog. In this study, we reconsider the long-lived aftershock hypothesis using rigorous tests assuming an Epidemic Type Aftershock Sequence (ETAS) model (*11*). ETAS modeling allows us to determine probabilities of observing robust features of the New Madrid catalog, should the long-lived aftershock hypothesis be true.

The ETAS model, developed on the premise that all earthquakes potentially trigger their own aftershocks, successfully explains the empirical Omori decay law, which, so far as is known, universally describes the temporal decay of aftershocks. The ETAS model explains observed foreshock rates and multiplets (*12*) and has been shown to accurately characterize seismicity, including both short- and long-term aftershock sequences [e.g., (*13*)], and is now a widely used short-term earthquake clustering model (*14*). The model has been used to characterize and forecast seismicity rates in a wide range of tectonic environments, including intraplate regions and regions characterized by swarmy activity (*15*, *16*). In this work, we use ETAS modeling in an attempt to generate synthetic catalogs that match well-constrained features of the New Madrid earthquake sequence (see materials and methods in the supplementary materials).

To test the long-lived aftershock hypothesis, we identified three robust observational constraints that are not dependent on particular contentious magnitude values. Our first imposed constraint

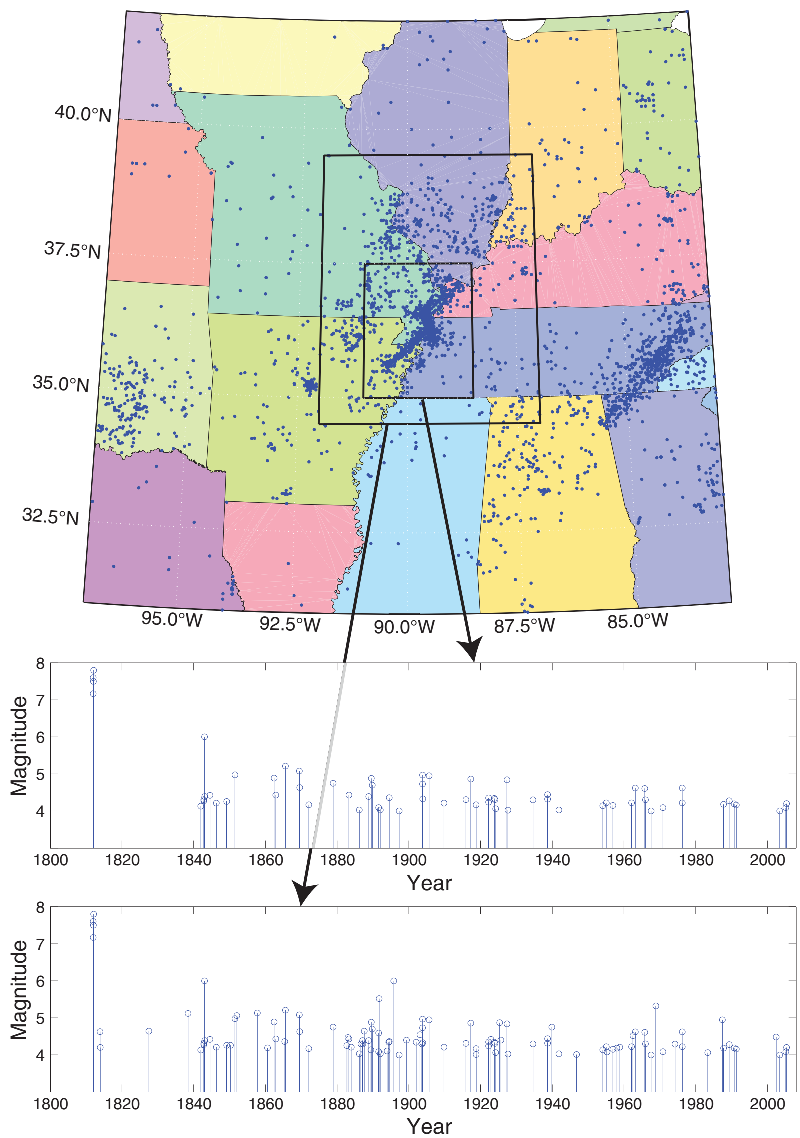

Fig. 1. Seismicity in the New Madrid region (CEUS catalog, 1800–2008, $M \geq 4$). Note that the early catalog is not complete to M4.

U.S. Geological Survey, Pasadena, CA, USA.
*Corresponding author. E-mail: pagem@caltech.edu

is that the sequence included four principal events of comparable magnitude, separated by no more than 0.7 magnitude units. This is based on the range in event magnitudes inferred by different studies (*2*, *3*, *17*). Although the absolute magnitudes of these earthquakes remain a subject for debate, the relative magnitudes are much more reliably determined. Analysis of prehistoric sandblows in the NMSZ shows that protracted sequences, with multiple large mainshocks, are apparently the norm for this region (*18*).

The second constraint is on the recent rate of moderate-sized ($M \geq 4$) earthquakes. Because using different catalogs and box sizes produce different estimates, we used the most conservative estimate of three $M \geq 4$ earthquakes over 10 years (Fig. 1), taken from the Central and Eastern United States Seismic Source Characterization (CEUS-SSC) catalog (*19*) (see materials and methods).

The third constraint is the number of moderate ($M \geq 6$) events in the NMSZ after the initial cluster in the first year. The CEUS-SSC catalog (*19*) includes two such events, the 1843 Marked Tree, Arkansas, and 1895 Charleston, Missouri, earthquakes, both with preferred magnitudes of 6.0. Although a recent reinterpretation of macroseismic effects of the 1843 earthquake (*20*) estimates a lower preferred magnitude of 5.4, we assume, for conservatism, that the sequence produced no more than two $M \geq 6$ late events (see materials and methods).

We generated synthetic ETAS catalogs, searching for a single set of subcritical, direct Omori parameters that matched the three robust observational constraints described above. The fraction of stochastic catalogs that are consistent with both early clustering behavior and recent seismicity in the New Madrid region are shown in Fig. 2, A and B, respectively. These two constraints reduce the possible ETAS phase space to a small region (Fig. 2C). Synthetic catalogs produced in this region of the ETAS phase space are very productive both early and late in the sequence. We find that synthetic sequences that are active enough to match observed New Madrid–style early clustering behavior and current seismicity rates contain many more $M \geq 6$ events at intermediate times than have been observed (table S1). At 95% confidence, no set of direct Omori parameters is consistent with all three of our constraints: early

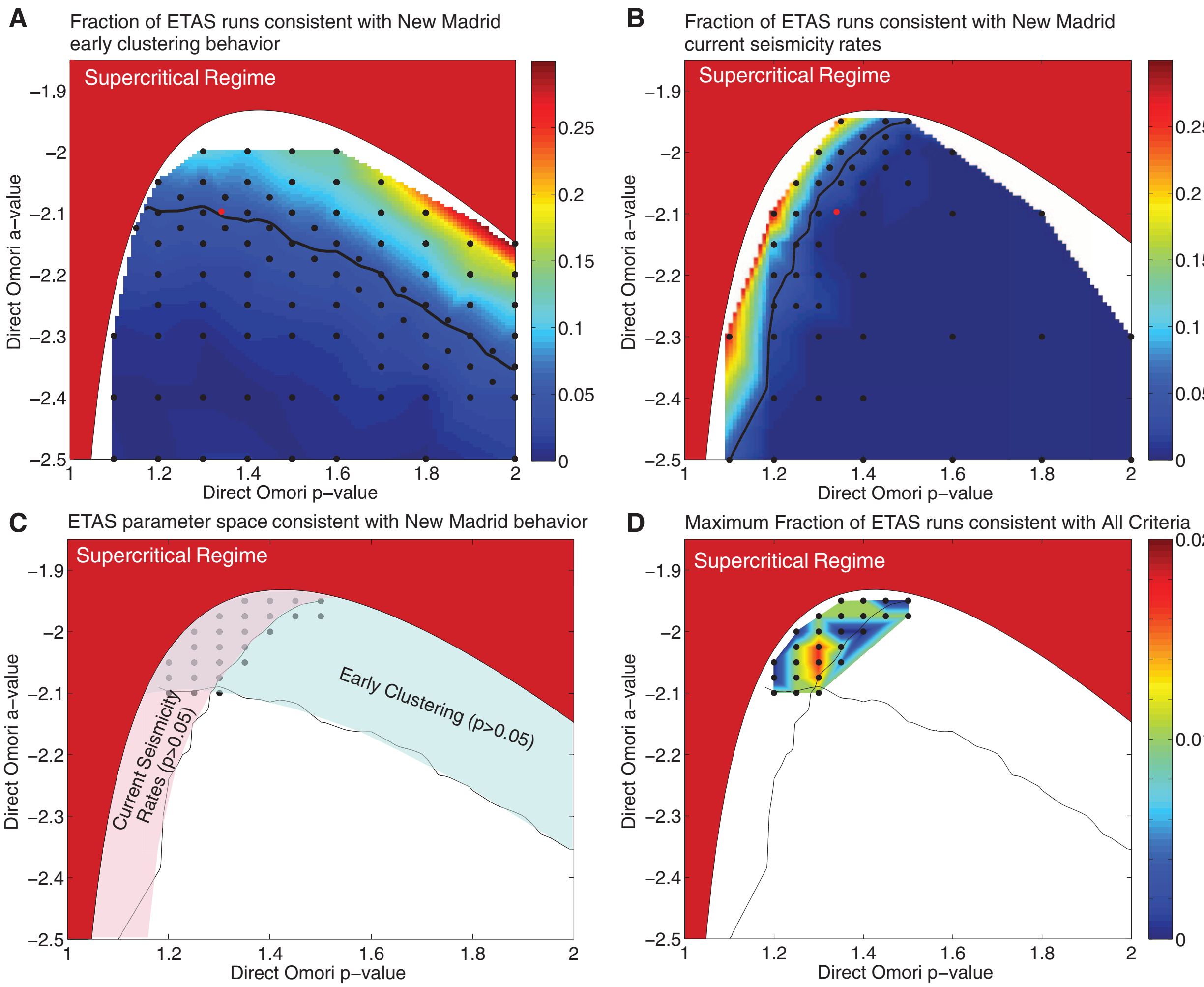

Fig. 2. Regions of ETAS parameter space consistent with New Madrid behavior. The unphysical, supercritical regime (see materials and methods) is shown in red. (**A**) ETAS simulations within the subcritical regime are sampled at the black points; colors show a linear interpolation of the fraction of synthetic sequences for which the four largest shocks in the first 2 months are within 0.7 magnitude units of each other, as was seen in the New Madrid sequence. Above the black line (which theoretically is smooth but has small irregularities due to sampling error), at least 5% of synthetic sequences are consistent with New Madrid clustering behavior; below this line, the early behavior is less productive than observations. The red dot shows average California parameters (*25*) for reference. (**B**) The fraction of synthetic sequences that have a late (200 years post-mainshock) aftershock rate that matches current New Madrid seismicity rates. (**C**) The parameter space consistent with both early clustering and current seismicity rates is confined to a small region; we sample sequences at the points shown and find that sequences with parameters in this region typically produce a much higher rate of *M*6 earthquakes after the first year than that observed. (**D**) The maximum fraction, over all mainshock magnitudes, that is consistent with early clustering, current seismicity rates, and the rate of $M \geq 6$ earthquakes after the first year, linearly interpolated between sampling points. Although some variation in this plot is due to sampling error, all points have been sampled sufficiently to determine that the fraction is less than 5%, at 95% confidence (see table S1).

clustering, current seismicity rates, and the rate of $M \geq 6$ events after the first year (Fig. 2D). Among sequences sampled that were consistent with New Madrid early clustering behavior and current seismicity rates, the mean number of $M \geq 6$ earthquakes from 1 year to 200 years post-mainshock was 135. At best, at some points in ETAS phase space ~1.7% of the sequences are consistent with our criteria. Results using a stricter criteria that includes the observation that no $M \geq 6$ earthquakes occurred in the region in the past 100 years (table S1) show that we can reject the long-lived aftershock hypothesis at even higher confidence.

Based on our statistical analysis, the hypothesis that current seismicity in the New Madrid region is primarily composed of aftershocks from the 1811–1812 sequence fails. This is because a sequence active enough at late times to produce the seismicity rates observed today and active enough at early times to produce the short-term clustering observed in the first few months would be highly likely to produce too many aftershocks in the intermediate times. If current seismicity in the New Madrid region is not composed predominantly of aftershocks, there must be continuing strain accrual. This is in agreement with recent work finding nonzero strain measurements in the region that are consistent with ongoing interseismic slip of about 4 mm/year (*21*), in contrast to earlier studies [e.g., (*22*)]. The spatial distribution of the stress pattern driven by this model would be generally consistent with the stress change caused by an earthquake on the Reelfoot fault. This could explain how ongoing microseismicity is not part of an aftershock sequence but is still consistent with the predicted stress change associated with the 1811–1812 sequence (*23*). If ongoing microseismicity does result from ongoing strain accrual, this suggests that the region, along with the neighboring Wabash Valley where nonzero strain has also been observed (*24*), will continue to be a source of hazard.

References and Notes

1. H. K. Gupta, N. P. Rao, B. K. Rastogi, D. Sarkar, *Science* **291**, 2101–2102 (2001).
2. S. E. Hough, M. Page, *J. Geophys. Res.* **116**, (B3), B03311 (2011).
3. A. C. Johnston, *Geophys. J. Int.* **126**, 314–344 (1996).
4. O. W. Nuttli, *Bull. Seismol. Soc. Am.* **63**, 227 (1973).
5. S. E. Hough, *Seismol. Res. Lett.* **80**, 1045–1053 (2009).
6. J. E. Ebel, K.-P. Bonjer, M. C. Oncescu, *Seismol. Res. Lett.* **71**, 283–294 (2000).
7. S. Stein, M. Liu, *Nature* **462**, 87–89 (2009).
8. F. Omori, *J. Coll. Sci. Imp. Univ. Tokyo* **7**, 111 (1895).
9. T. Utsu, *Geophys. Mag.* **30**, 521 (1961).
10. T. Utsu, Y. Ogata, R. S. Matsu'ura, *J. Phys. Earth* **43**, 1–33 (1995).
11. Y. Ogata, *J. Am. Stat. Assoc.* **83**, 9–27 (1988).
12. K. R. Felzer, R. E. Abercrombie, G. Ekstršm, *Bull. Seismol. Soc. Am.* **94**, 88–98 (2004).
13. Y. Ogata, *J. Geophys. Res.* **97**, (B13), 19845 (1992).
14. M. C. Gerstenberger, D. A. Rhoades, *Pure Appl. Geophys.* **167**, 877–892 (2010).
15. Y. Ogata, J. Zhuang, *Tectonophysics* **413**, 13–23 (2006).
16. A. L. Llenos, J. J. McGuire, Y. Ogata, *Earth Planet. Sci. Lett.* **281**, 59–69 (2009).
17. W. H. Bakun, M. G. Hopper, *Bull. Seismol. Soc. Am.* **94**, 64–75 (2004).
18. M. P. Tuttle, *Bull. Seismol. Soc. Am.* **92**, 2080–2089 (2002).
19. K. J. Coppersmith *et al*., Central and Eastern United States Seismic Source Characterization for Nuclear Facilities Project, Technical Report (Electric Power Research Institute, Palo Alto, CA, 2012).
20. S. E. Hough, *Bull. Seismol. Soc. Am.* **103**, 2767 (2013).
21. A. Frankel, R. Smalley, J. Paul, *Bull. Seismol. Soc. Am.* **102**, 479–489 (2012).
22. E. Calais, J. Y. Han, C. DeMets, J. M. Nocquet, *J. Geophys. Res.* **111**, (B6), 6402 (2006).
23. K. Mueller, S. E. Hough, R. Bilham, *Nature* **429**, 284–288 (2004).
24. G. A. Galgana, M. W. Hamburger, *Seismol. Res. Lett.* **81**, 699–714 (2010).
25. K. R. Felzer, R. E. Abercrombie, G. Ekström, *Bull. Seismol. Soc. Am.* **93**, 1433–1448 (2003).

Acknowledgments: We thank J. Hardebeck, C. Mueller, and two anonymous reviewers for comments on the manuscript. The CEUS-SSC catalog is available at: www.ceus-ssc.com/Report/Downloads.html. Author Contributions: M.T.P. did the ETAS modeling, and S.E.H. provided expertise on the historical catalog. Both authors participated in the writing.

Supplementary Materials

www.sciencemag.org/content/343/6172/762/suppl/DC1
Materials and Methods
Fig. S1
Table S1
References (*26*–*30*)

7 November 2013; accepted 15 January 2014
Published online 23 January 2014;
10.1126/science.1248215

www.sciencemag.org/cgi/content/full/science.1248215/DC1

Supplementary Materials for

The New Madrid Seismic Zone: Not Dead Yet

Morgan T. Page* and Susan E. Hough

*To whom correspondence should be addressed. E-mail: pagem@caltech.edu

Published 23 January 2014 on *Science* Express
DOI: 10.1126/science.1248215

This PDF file includes:

Materials and Methods
Fig. S1
Table S1
References

Materials and Methods

It is well-known that the rate of aftershocks with time can be fit by the Omori law, as modified by Utsu:

$$R(t) = \frac{K}{(c+t)^p}, \tag{1}$$

where t is the time since the mainshock, and K, c, and p are constants with p typically around 1 (*8, 9*). This law is also termed the *indirect* Omori Law, as it includes not only aftershocks triggered directly by the mainshock, but also secondary aftershocks triggered by those primary aftershocks. Successive modeling of each generation of aftershocks is the idea behind Epidemic Type Aftershock Sequence (ETAS) modeling (*11*), in which each earthquake in a sequence triggers subsequent earthquakes at a rate

$$R(t) = \frac{10^{a+b(M-M_{min})}}{(c+t)^p}, \tag{2}$$

where M is the magnitude of the triggering earthquake, M_{min} is the minimum magnitude under consideration, and b is the Gutenberg-Richter b-value. Note that the constants a, p, c are the *direct* Omori constants and differ from the parameters in the indirect Omori Law from Equation 1. When the direct Omori Law is summed up over all generations of aftershocks, it approximately gives the indirect law, although at short times the p-value for the total sequence will be less than the direct p-value (*26*).

If the magnitude distribution of aftershocks is given by the Gutenberg-Richter magnitude distribution (*27*) truncated at a maximum magnitude of M_{max}, then the mean number of aftershocks triggered from each earthquake is given by the branching ratio

$$n = \frac{10^{a+bM_{max}} bc^{1-p}(M_{max} - M_{min})log(10)}{10^{bM_{max}} - 10^{bM_{min}}(p-1)}, \quad (3)$$

as described Sornette and Sornette (*28*). In the supercritical regime $n > 1$, each generation of aftershocks produces, on average, more subsequent aftershocks than the previous generation, leading to an eventual unphysical, exponential increase in the seismicity rate (*29*).

We produce synthetic ETAS catalogs for different values of a and p, searching for regions in the parameter space that can produce catalogs that have similar characteristics to the observed New Madrid catalog. In our ETAS modeling, we assume a b-value of 1.0, which fits central U.S. seismicity well (*19*), and a c-value of 0.095 days that has been derived from ETAS fits to California seismicity (*25*) (for the time scales we are considering here, results are not sensitive to this parameter). We generate synthetic catalogs down to a minimum magnitude M_{min} of 2.5. Since we are trying to generate catalogs that are consistent with the hypothesis that recent earthquakes in the New Madrid region are aftershocks of the 1811-1812 events, we do not add background (spontaneously triggered) events to the ETAS simulations.

As discussed in the main text, one of the observational constraints we attempt to match in our ETAS modeling is the modern rate of $M \geq 4$ earthquakes in the New Madrid region. The CEUS-SSC catalog (*19*) contains 3 and 6 $M \geq 4$ earthquakes for a small and large box around the NMSZ (see Fig. 1), respectively, in the last 10 years of the catalog (1998-2008). The ANSS catalog has 5 and 8 $M \geq 4$ earthquakes for these two regions for the last 10 years (2003-2013). Given the difficulty in choosing the appropriate size of box for the NMSZ and the differences between the catalogs, our philosophy is to make choices that give the long-lived aftershock hypothesis the best chance of succeeding. We thus use the constraint of 3 $M \geq 4$ earthquakes over 10 years for the current seismicity rate, since higher rates will require a more productive aftershock sequence and more strict bounds on the allowed ETAS parameters.

We also include a constraint on the number of $M \geq 6$ earthquakes after 1812. For this constraint, catalog completeness is a potential consideration. Hough (*5*) shows that, even during the early sequence, events as low as $M6-6.5$ can be identified based on the archival record; however, clearly the catalog of early large aftershocks could be incomplete. However, while searches of available on-line compilations of historical newspapers reveal a steady sprinkling of felt reports in the central/eastern U.S. as far back as spring, 1812, there is no evidence for any widely felt events after March, 1812. The first widely felt event after 1812 is the 1843 Marked Tree, Arkansas earthquake. Given the well-established low intensity attenuation in the Central U.S. [*e.g.*, (*30*)], moderate earthquakes are very widely felt. Reports from the USGS "Did You Feel It?" system show that the 2008 $M_w5.2$ Mt Carmel, Illinois, earthquake was felt to a distance of 500 km, with sparse felt reports from distances upwards of 1000 km. The 2011 $M_w5.8$ Mineral, Virginia earthquake was felt to 1000 km, with sparse felt reports extending to over 1500 km. Even weakly felt earthquakes were reported by 19$^{\text{th}}$ century newspapers. It is thus highly improbable that a NMSZ event as large as $M5$, let alone 6, went undocumented between 1812 and 1900. Therefore, we look for synthetic catalogs that have no more the 2 $M \geq 6$ earthquakes after 1812, which allows for the possibility that the the 1843 Marked Tree, Arkansas, and 1895 Charleston, Missouri, earthquakes could be as large as $M6$.

In Fig. S1, we show example catalogs using the ETAS parameters for which the largest percentage of catalogs match our observational constraints. The aftershock rate for these ETAS catalogs typically drops below current New Madrid seismicity rates in the first few decades.

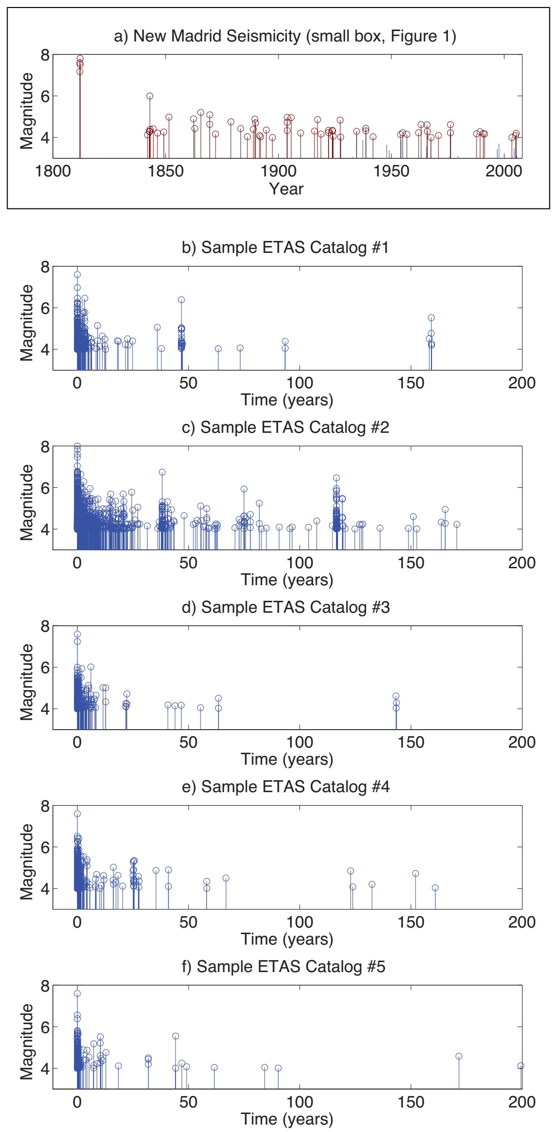

Figure S1: **The New Madrid catalog compared to sample ETAS catalogs.** a) Seismicity in the New Madrid region (small box in Fig. 1, CEUS catalog, 1800-2008, $M \geq 4$). Note that the early catalog is not complete to $M4$. b-f) $M \geq 4$ earthquakes from five synthetic ETAS catalogs with a=-2.05, p=1.3, and mainshock magnitude $M_{main} = 7.6$. These are the ETAS parameters that come closest to matching the observational constraints.

TABLE S1: **ETAS Sampling Results**. Each point has been sampled sufficiently to ensure that less than 5% of the sequences are consistent with New Madrid short-term clustering, current seismicity rates, and the $M6$ rate after the first year, at 95% confidence.

p-value	a-value	Mainshock Magnitude	Number of Samples	Number Consistent with Short-term Clustering and Current Seismicity Rate	Number Consistent with Short-term Clustering, Current seismicity Rate, and M6 Rate (Years 1-200)	Percent Consistent with Short-term Clustering, Current seismicity Rate, and M6 Rate (Years 1-200)	Number Consistent with Short-term Clustering, Current Seismicity Rate, and M6 Rate (Years 1-100, 101-200)	Percent Consistent with Short-term Clustering, Current Seismicity Rate, and M6 Rate (Years 1-100, 101-200)
1.20	-2.100	8.0	100	5	0	0.0	0	0.0
1.20	-2.075	8.0	100	7	0	0.0	0	0.0
1.20	-2.050	8.0	100	5	0	0.0	0	0.0
1.25	-2.100	8.0	100	5	0	0.0	0	0.0
1.25	-2.075	8.0	100	6	0	0.0	0	0.0
1.25	-2.050	8.0	100	3	0	0.0	0	0.0
1.25	-2.025	8.0	100	5	0	0.0	0	0.0
1.25	-2.000	8.0	100	16	0	0.0	0	0.0
1.30	-2.100	8.0	100	2	0	0.0	0	0.0
1.30	-2.075	8.0	100	4	1	1.0	1	1.0
1.30	-2.050	8.0	100	1	0	0.0	0	0.0
1.30	-2.025	8.0	100	10	0	0.0	0	0.0
1.30	-2.000	8.0	100	9	0	0.0	0	0.0
1.30	-1.975	8.0	100	19	0	0.0	0	0.0
1.35	-2.050	8.0	100	1	0	0.0	0	0.0
1.35	-2.025	8.0	100	4	0	0.0	0	0.0
1.35	-2.000	8.0	100	6	0	0.0	0	0.0
1.35	-1.975	8.0	100	15	0	0.0	0	0.0
1.35	-1.950	8.0	100	21	0	0.0	0	0.0
1.40	-2.000	8.0	100	3	0	0.0	0	0.0
1.40	-1.975	8.0	100	11	0	0.0	0	0.0
1.40	-1.950	8.0	100	20	0	0.0	0	0.0
1.45	-1.975	8.0	100	7	0	0.0	0	0.0
1.45	-1.950	8.0	100	21	0	0.0	0	0.0
1.50	-1.975	8.0	100	6	0	0.0	0	0.0
1.50	-1.950	8.0	100	9	0	0.0	0	0.0
1.20	-2.100	7.6	100	6	1	1.0	1	1.0
1.20	-2.075	7.6	100	4	0	0.0	0	0.0
1.20	-2.050	7.6	100	3	0	0.0	0	0.0
1.25	-2.100	7.6	100	3	1	1.0	1	1.0
1.25	-2.075	7.6	100	2	0	0.0	0	0.0
1.25	-2.050	7.6	100	2	0	0.0	0	0.0
1.25	-2.025	7.6	100	10	1	1.0	0	0.0
1.25	-2.000	7.6	100	11	0	0.0	0	0.0
1.30	-2.100	7.6	200	4	2	1.0	2	1.0
1.30	-2.075	7.6	200	6	3	1.5	2	1.0
1.30	-2.050	7.6	300	13	5	1.7	4	1.3
1.30	-2.025	7.6	300	18	5	1.7	5	1.7

Continued on next page

TABLE S1 – continued from previous page

p-value	a-value	Mainshock Magnitude	Number of Samples	Number Consistent with Short-term Clustering and Current Seismicity Rate	Number Consistent with Short-term Clustering, Current seismicity Rate, and M6 Rate (Years 1-200)	Percent Consistent with Short-term Clustering, Current seismicity Rate, and M6 Rate (Years 1-200)	Number Consistent with Short-term Clustering, Current Seismicity Rate, and M6 Rate (Years 1-100, 101-200)	Percent Consistent with Short-term Clustering, Current Seismicity Rate, and M6 Rate (Years 1-100, 101-200)
1.30	-2.000	7.6	300	36	3	1.0	2	0.7
1.30	-1.975	7.6	300	55	3	1.0	3	1.0
1.35	-2.050	7.6	200	4	1	0.5	1	0.5
1.35	-2.025	7.6	200	4	0	0.0	0	0.0
1.35	-2.000	7.6	100	2	0	0.0	0	0.0
1.35	-1.975	7.6	300	24	3	1.0	3	1.0
1.35	-1.950	7.6	300	37	3	1.0	1	0.3
1.40	-2.000	7.6	100	5	0	0.0	0	0.0
1.40	-1.975	7.6	200	11	2	1.0	2	1.0
1.40	-1.950	7.6	100	17	1	1.0	1	1.0
1.45	-1.975	7.6	100	3	1	1.0	1	1.0
1.45	-1.950	7.6	100	9	0	0.0	0	0.0
1.50	-1.975	7.6	100	0	0	0.0	0	0.0
1.20	-2.100	7.2	100	0	0	0.0	0	0.0
1.20	-2.075	7.2	100	4	0	0.0	0	0.0
1.20	-2.050	7.2	100	7	0	0.0	0	0.0
1.25	-2.100	7.2	100	0	0	0.0	0	0.0
1.25	-2.075	7.2	200	5	2	1.0	2	1.0
1.25	-2.050	7.2	100	2	1	1.0	1	1.0
1.25	-2.025	7.2	100	6	0	0.0	0	0.0
1.25	-2.000	7.2	100	3	0	0.0	0	0.0
1.30	-2.100	7.2	100	0	0	0.0	0	0.0
1.30	-2.075	7.2	100	1	0	0.0	0	0.0
1.30	-2.050	7.2	100	2	1	1.0	1	1.0
1.30	-2.025	7.2	100	2	0	0.0	0	0.0
1.30	-2.000	7.2	100	4	1	1.0	1	1.0
1.30	-1.975	7.2	100	3	0	0.0	0	0.0
1.35	-2.050	7.2	100	0	0	0.0	0	0.0
1.35	-2.025	7.2	100	0	0	0.0	0	0.0
1.35	-2.000	7.2	100	0	0	0.0	0	0.0
1.35	-1.975	7.2	100	7	1	1.0	1	1.0
1.35	-1.950	7.2	100	5	1	1.0	1	1.0
1.40	-2.000	7.2	100	1	0	0.0	0	0.0
1.40	-1.975	7.2	100	1	0	0.0	0	0.0
1.40	-1.950	7.2	100	9	1	1.0	0	0.0
1.45	-1.975	7.2	100	1	1	1.0	1	1.0
1.45	-1.950	7.2	100	0	0	0.0	0	0.0
1.50	-1.975	7.2	100	0	0	0.0	0	0.0
1.50	-1.950	7.2	100	4	0	0.0	0	0.0
1.20	-2.100	6.8	100	0	0	0.0	0	0.0
1.20	-2.075	6.8	100	0	0	0.0	0	0.0

Continued on next page

TABLE S1 – continued from previous page

p-value	a-value	Mainshock Magnitude	Number of Samples	Number Consistent with Short-term Clustering and Current Seismicity Rate	Number Consistent with Short-term Clustering, Current seismicity Rate, and M6 Rate (Years 1-200)	Percent Consistent with Short-term Clustering, Current seismicity Rate, and M6 Rate (Years 1-200)	Number Consistent with Short-term Clustering, Current Seismicity Rate, and M6 Rate (Years 1-100, 101-200)	Percent Consistent with Short-term Clustering, Current Seismicity Rate, and M6 Rate (Years 1-100, 101-200)
1.20	-2.050	6.8	100	3	0	0.0	0	0.0
1.25	-2.100	6.8	100	0	0	0.0	0	0.0
1.25	-2.075	6.8	100	2	1	1.0	1	1.0
1.25	-2.050	6.8	100	0	0	0.0	0	0.0
1.25	-2.025	6.8	100	2	0	0.0	0	0.0
1.25	-2.000	6.8	100	4	0	0.0	0	0.0
1.30	-2.100	6.8	100	0	0	0.0	0	0.0
1.30	-2.075	6.8	100	0	0	0.0	0	0.0
1.30	-2.050	6.8	100	1	1	1.0	0	0.0
1.30	-2.025	6.8	100	0	0	0.0	0	0.0
1.30	-2.000	6.8	100	3	0	0.0	0	0.0
1.30	-1.975	6.8	100	3	0	0.0	0	0.0
1.35	-2.050	6.8	100	0	0	0.0	0	0.0
1.35	-2.025	6.8	100	1	1	1.0	1	1.0
1.35	-2.000	6.8	100	0	0	0.0	0	0.0
1.35	-1.975	6.8	100	2	0	0.0	0	0.0
1.35	-1.950	6.8	100	2	0	0.0	0	0.0
1.40	-2.000	6.8	100	0	0	0.0	0	0.0
1.40	-1.975	6.8	100	0	0	0.0	0	0.0
1.40	-1.950	6.8	100	5	0	0.0	0	0.0
1.45	-1.975	6.8	100	0	0	0.0	0	0.0
1.45	-1.950	6.8	100	0	0	0.0	0	0.0
1.50	-1.975	6.8	100	3	1	1.0	1	1.0
1.50	-1.950	6.8	100	2	0	0.0	0	0.0

References

1. H. K. Gupta, N. P. Rao, B. K. Rastogi, D. Sarkar, The deadliest intraplate earthquake. *Science* **291**, 2101–2102 (2001). doi:10.1126/science.1060197 Medline

2. S. E. Hough, M. Page, Toward a consistent model for strain accrual and release for the New Madrid Seismic Zone, central United States. *J. Geophys. Res.* **116**, (B3), B03311 (2011). doi:10.1029/2010JB007783

3. A. C. Johnston, Seismic moment assessment of earthquakes in stable continental regions-III. New Madrid 1811-1812, Charleston 1886 and Lisbon 1755. *Geophys. J. Int.* **126**, 314–344 (1996). doi:10.1111/j.1365-246X.1996.tb05294.x

4. O. W. Nuttli, *Bull. Seismol. Soc. Am.* **63**, 227 (1973).

5. S. E. Hough, Cataloging the 1811-1812 New Madrid, Central U.S., Earthquake Sequence. *Seismol. Res. Lett.* **80**, 1045–1053 (2009). doi:10.1785/gssrl.80.6.1045

6. J. E. Ebel, K.-P. Bonjer, M. C. Oncescu, Paleoseismicity: Seismicity evidence for past large earthquakes. *Seismol. Res. Lett.* **71**, 283–294 (2000). doi:10.1785/gssrl.71.2.283

7. S. Stein, M. Liu, Long aftershock sequences within continents and implications for earthquake hazard assessment. *Nature* **462**, 87–89 (2009). doi:10.1038/nature08502 Medline

8. F. Omori, *J. Coll. Sci. Imp. Univ. Tokyo* **7**, 111 (1895).

9. T. Utsu, *Geophys. Mag.* **30**, 521 (1961).

10. T. Utsu, Y. Ogata, R. S. Matsu'ura, The centenary of the Omori Formula for a decay law of aftershock activity. *J. Phys. Earth* **43**, 1–33 (1995). doi:10.4294/jpe1952.43.1

11. Y. Ogata, Statistical models for earthquake occurrences and residual analysis for point processes. *J. Am. Stat. Assoc.* **83**, 9–27 (1988). doi:10.1080/01621459.1988.10478560

12. K. R. Felzer, R. E. Abercrombie, G. Ekstršm, A common origin for aftershocks, foreshocks, and multiplets. *Bull. Seismol. Soc. Am.* **94**, 88–98 (2004). doi:10.1785/0120030069

13. Y. Ogata, Detection of precursory relative quiescence before great earthquakes through a statistical model. *J. Geophys. Res.* **97**, (B13), 19845 (1992). doi:10.1029/92JB00708

14. M. C. Gerstenberger, D. A. Rhoades, New Zealand Earthquake Forecast Testing Centre. *Pure Appl. Geophys.* **167**, 877–892 (2010). doi:10.1007/s00024-010-0082-4

15. Y. Ogata, J. Zhuang, Space-time ETAS models and an improved extension. *Tectonophysics* **413**, 13–23 (2006). doi:10.1016/j.tecto.2005.10.016

16. A. L. Llenos, J. J. McGuire, Y. Ogata, Modeling seismic swarms triggered by aseismic transients. *Earth Planet. Sci. Lett.* **281**, 59–69 (2009). doi:10.1016/j.epsl.2009.02.011

17. W. H. Bakun, M. G. Hopper, Magnitudes and locations of the 1811-1812 New Madrid, Missouri, and the 1886 Charleston, South Carolina, earthquakes. *Bull. Seismol. Soc. Am.* **94**, 64–75 (2004). doi:10.1785/0120020122

18. M. P. Tuttle, The earthquake potential of the New Madrid Seismic Zone. *Bull. Seismol. Soc. Am.* **92**, 2080–2089 (2002). doi:10.1785/0120010227

19. K. J. Coppersmith *et al*., Central and eastern United States (CEUS) seismic source characterization (SSC) for nuclear facilities project, *Tech. rep.*, Electric Power Research Institute (EPRI) (2012).

20. S. E. Hough, Spatial variability of "Did you feel it?" intensity data: Insights into sampling biases in historical earthquake intensity distributions. *Bull. Seismol. Soc. Am.* **103**, 2767 (2013). doi:10.1785/0120120285

21. A. Frankel, R. Smalley, J. Paul, Significant motions between GPS Sites in the New Madrid region: Implications for seismic hazard. *Bull. Seismol. Soc. Am.* **102**, 479–489 (2012). doi:10.1785/0120100219

22. E. Calais, J. Y. Han, C. DeMets, J. M. Nocquet, Deformation of the North American plate interior from a decade of continuous GPS measurements. *J. Geophys. Res.* **111**, (B6), 6402 (2006). doi:10.1029/2005JB004253

23. K. Mueller, S. E. Hough, R. Bilham, Analysing the 1811-1812 New Madrid earthquakes with recent instrumentally recorded aftershocks. *Nature* **429**, 284–288 (2004). doi:10.1038/nature02557 Medline

24. G. A. Galgana, M. W. Hamburger, Geodetic observations of active intraplate crustal deformation in the Wabash Valley Seismic Zone and the Southern Illinois Basin. *Seismol. Res. Lett.* **81**, 699–714 (2010). doi:10.1785/gssrl.81.5.699

25. K. R. Felzer, R. E. Abercrombie, G. Ekstršm, Secondary aftershocks and their importance for aftershock forecasting. *Bull. Seismol. Soc. Am.* **93**, 1433–1448 (2003). doi:10.1785/0120020229

26. A. Helmstetter, D. Sornette, Importance of direct and indirect triggered seismicity in the ETAS model of seismicity. *Geophys. Res. Lett.* **30**, 1576 (2003). doi:10.1029/2003GL017670

27. B. Gutenberg, C. F. Richter, *Bull. Seismol. Soc. Am.* **4**, 185 (1944).

28. A. Sornette, D. Sornette, Renormalization of earthquake aftershocks. *Geophys. Res. Lett.* **26**, 1981–1984 (1999). doi:10.1029/1999GL900394

29. A. Helmstetter, D. Sornette, Subcritical and supercritical regimes in epidemic models of earthquake aftershocks. *J. Geophys. Res.* **107**, (B10), 2237 (2002). doi:10.1029/2001JB001580

30. A. C. Johnston, Seismic moment assessment of earthquakes in stable continental regions-I. Instrumental seismicity. *Geophys. J. Int.* **124**, 381–414 (1996). doi:10.1111/j.1365-246X.1996.tb07028.x